2023 IEEE International Conference on Robotics and Automation (ICRA 2023)
May 29 - June 2, 2023. London, UK

Mechanical Intelligence for Prehensile In-Hand Manipulation of Spatial Trajectories

Qiujie Lu[1,2], Zhongxue Gan[1], Xinran Wang[2], Guochao Bai[3], Zhuang Zhang[4] and Nicolas Rojas[2]

***Abstract*— The application of mechanical and other physical properties to the development of robotic systems that can easily adapt to changing external situations is known as mechanical intelligence. Following this concept, many robot hand designs can produce self-adaptive and versatile grasps with simple underactuated fingers and open-loop control, while mechanical-intelligent strategies for dexterous manipulation are still limited. This paper proposes a mechanical-intelligent technique to facilitate dexterous manipulation, in particular prehensile in-hand manipulation. The proposed strategy is based on the generation of complex spatial trajectories of the hand-object system, controlled in open loop with the minimum number of actuators and using simple low-level non-position modes. This approach is exemplified by the rigorous analysis and testing of a three-fingered two-actuator underactuated robot hand, called the helical hand, which is capable of generating helical prehensile in-hand manipulation of diversiform objects under error tolerance controlled by constant speed algorithm.**

I. Introduction

Robots are becoming more prevalent in our daily life for assisting with people in a variety of environments. However, despite this trend and the substantial progress made in the last 40 years, and particularly recently using deep reinforcement learning techniques—e.g., [1], [2], performing reliable dexterous manipulation operations under both shape diversity and shape uncertainty with a robot hand is still an open question [3]. Further research is indeed needed in the components of a dexterous manipulation robotic system, which are a robotic hand and a control policy, along with the object to be grasped and manipulated by the hand [4].

In the case of robotic hands, research in their design has been historically dominated by efforts that focus on the hand solely, with the purpose of developing manipulation systems that are suitable for arbitrary objects. The sophistication of current designs indeed diverges enormously, from single degree of freedom parallel jaw grippers [5] to complex anthropomorphic hands with a high number of degrees of freedom (e.g., DLR [6], Gifu [7], Shadow [8]). There are, nonetheless, many other hand designs in the midst of these extremes that utilized a small number of actuators or combined passive and coupled degrees of freedom [9], [10]. For instance, underactuated hands, by actuating multiple hand phalanges with a single actuator through a carefully designed transmission mechanism, are relatively simple to control while being able to grasp diverse objects [11], [12]. Nevertheless, the ability of these hands to perform complex tasks and in-hand manipulation operations, despite recent progress [13], is still very limited, and their transition from grasping control to dexterous manipulation control has shown to break the simplicity of the former. Previously, [14] explored a self-adaptive precision grasping of this robot hand. This research mainly investigates complex in-hand manipulation motion of spatial trajectories with the help of machine intelligence.

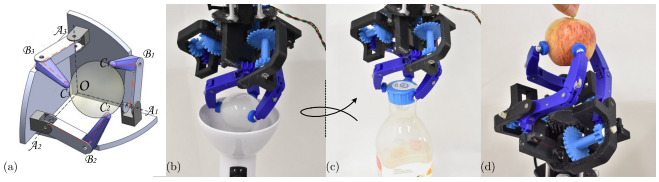

Fig. 1. **(a)** Kinematic structure of the helical hand: three fingers attached to three orthogonal planes. Examples of helical prehensile in-hand manipulations applications with the helical hand: screwing a light bulb **(b)**, unscrewing a bottle lid **(c)**, and removing the stem of an apple by twisting and pulling **(d)**.

Dexterous in-hand manipulation broadens the utility of the hand for not only acquiring and maintaining grasps but also for allowing fine adjustments to the position and orientation of the grasped object. This re-positioning is called precision in-hand manipulation when it occurs without breaking or changing the contact between each fingertip and the object [15], but the notion of in-hand manipulation is certainly broader [16]. Some robotic hands exploiting mechanical intelligence have been developed to facilitate in-hand manipulation. For example, the GR2 gripper [17] is a two-fingered hand that introduces an elastic pivot joint between the fingers to enlarge the range of planar reorientation. [18] designed an intelligent embodied tendon-driven mechanism based on turning transmission friction from a disturbance into a design tool to perform a variety of grasping and manipulation tasks. [19] proposed a three-fingered gripper that is actuated by a single motor and is able to grasp objects and perform rolling manipulation with a working mode switching mechanism. Recently, a three-finger robot hand

This work was supported by Shanghai Pujiang Program, Shanghai Municipal Science and Technology Major Project (No.2021SHZDZX0103), Shanghai Engineering Research Center of AI Robotics, Fudan University, China., Engineering Research Center of AI Robotics, Ministry of Education, China., an Amazon Research Award ,and the Engineering and Physical Sciences Research Council grant EP/R020833/1.

[1]Academy for Engineering and Technology, Fudan University, 200433, Shanghai, China. (e-mail: {qj_lu, ganzhongxue}@fudan.edu.cn)

[2]REDS Lab, Dyson School of Design Engineering, Imperial College London, 25 Exhibition Road, London SW7 2DB, UK. (e-mail: {q.lu17, xinran.wang20, n.rojas}@imperial.ac.uk)

[3]ChangingTek Ltd, Wangjing Science & Technology Innovation Park, Chaoyang District, Beijing 100102, China.

[4]School of Engineering, Westlake University, Hangzhou, 310030, China

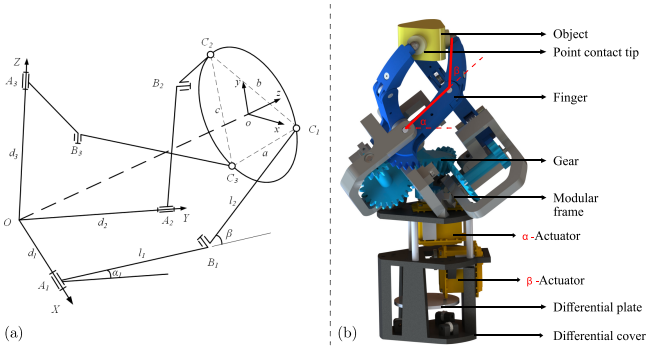

Fig. 2. **(a)** Schematic view of the hand-object system with global coordinate systems O-XYZ and object coordinate system o-xyz. **(b)** CAD model of the proposed helical hand.

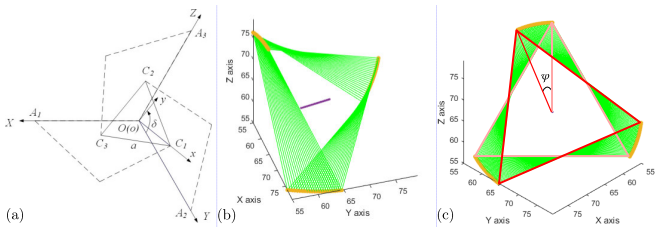

Fig. 3. **(a)** Top view of the hand- object system. δ is the rotation angle between the reference frames $\{\mathrm{m}\}$ and $\{\mathrm{B}\}$. Simulation of the helical motion trajectory of a triangular object of size 30 mm based on the actual prototype's actuation range **(b & c)**. The coloured circles are the contact point positions of each finger, the purple dots indicate the centre point of the equilateral triangle. ψ indicates the object rotation range from the starting to the end position.

with a reconfigurable palm utilised two five-bar linkages to create systematic prehensile in-hand manipulations [20].

Most of the underactuated hands are limited to perform in-hand manipulation in a planar plane [21] [22]. For more complex or spatial dexterous in-hand manipulations, researchers have preferred to create or use anthropomorphic hands [23]. OpenAI [1] used deep reinforcement learning to learn dexterous in-hand manipulation to perform vision-based object reorientation on a Shadow Hand. The hand was taking advantage of gravity to accomplish the object reorientation where the object can rest on the palm without grasping, this is indeed a tendency in other similar works (e.g., [24]). The i-HY Hand [25] which is an underactuated hand can achieve a wide range of grasping and in-hand manipulation tasks, but it requires proper evaluation and modelling for each object geometry.

Unscrewing and screwing objects is essential for humans, but reproducing such manipulation behaviour requires detailed knowledge about the object position, contact location with sensor feedback and redundant control systems. Research on prehensile in-hand helical manipulation trajectories remains an open problem in the dexterous manipulation literature. Examples of these approaches are [26] and [27], where bioinspired sinusoidal finger joint synergies and electrocardiogram synergy control of an anthropomorphic artificial hand were used. [28] proposed a simpler solution based on a soft robotic gripper that can twist objects but it requires 3 pneumatic chambers per each finger. [29] recently developed a deep reinforcement learning algorithm for some related everyday hand manipulations such as valve rotation, box flipping, and opening a door with flexible handle using a three-fingered simple hand, but these operations, as set by the authors, do not require prehensile motions. Solutions proposed for twisting and pulling [Fig. 1(c)], which is another type of prehensile helical motion, were not identified.

In this paper, we explored the mechanical intelligence of our underactuated robot hand, with simple velocity control, which can achieve helical in-hand manipulation motion with different sizes and shapes of objects. In section II, the helical motion is thoroughly analysed using a mathematical model to gain insight into this type of manipulation. From this model, section III presents a low-level control scheme and detailed kinematic analysis of the robotic hand. The actuation method and fingertip design are then defined based on these results. Experiment results of our robot hand's prehensile helical in-hand motion are demonstrated in section IV. Lastly, we discuss the helical hand's performance and limitations as well as future developments.

II. In-Hand Manipulation Analysis of Grasped Objects

A. Design of the Helical Hand

Figure 1(a) shows the kinematic structure of the helical hand. The robotic hand consists of three fingers, each finger is composed of two parallel revolute joints. The fingers are attached to three orthogonal planes, where the proximal joint axes are perpendicular to each other.

According to the extended Chebychev-Kutzbach-Grübler criterion, for the hand-object system of the helical hand we have the mobility of the hand-object system for the helical hand (under the point contact with friction assumption) is 3, the feasible movements of a manipulated object correspond to a three-manifold. The helical hand consists of two actuators for grasping and manipulation. One actuator for the three proximal joints and one actuator for the three distal joints. This makes the hand-object system underactuated.

Figure 2(b) shows the CAD view of the helical hand which is designed based on the topology of the underactuated hand-object system. The hand is mainly divided into two parts: the top part is a cubic structure based finger system and the bottom part is the actuation and the differential system. The actuation range of the proximal joints and distal joints are from -48^o to 7^o and 75^o to 107^o respectively. More detailed information of the prototype can be found in [14].

B. Kinematic Analysis of Manipulation Phase

The following kinematic analysis can find the manipulation trajectory of the grasped objects based on the schematic view of the hand-object system 2(a). The orientation of the object with respect to the base frame $\{\mathrm{B}\}$ is given by a orientation matrix R. For the analysed hand dimensions

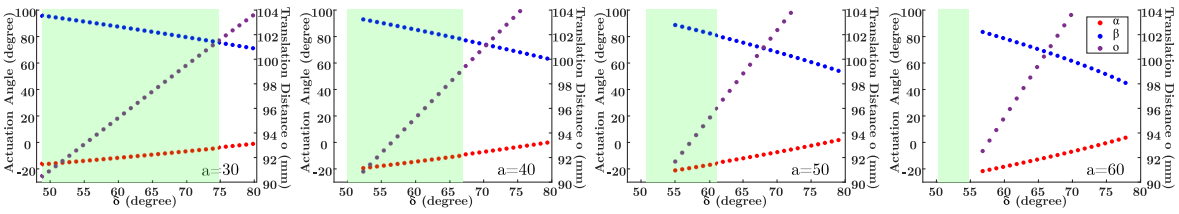

Fig. 4. The relationship between the actuation angle α, β (°), the translation distance o (mm) and the orientation δ with different object sizes a (mm). Green areas indicate the feasible rotation range of each object.

($d_1 = d_2 = d_3 = l_1 = l_2 = 55mm$), the {m} coordinate system o-xyz needs to rotate three times to fit the global coordinate system O-XYZ. Firstly, a rotation along the Z-axis of θ_1=45^o. Then, a rotation along the X-axis of θ_2=54.736^o. Finally, a rotation along the Z-axis of $\theta_3 = \delta$+60^o, where δ is the rotational angle between the Y-axis and y-axis (the orientation of the object) as shown in Fig. 3(a). Therefore, the corresponding orientation matrix R can be worked out.

In the in-hand manipulation analysis, the manipulated body is an equilateral triangular object, where the edge lengths are the same, so the coordinates of the points C_i in {m} can be simplified as $C_1^{'} = [\frac{\sqrt{3}}{3}a, 0, 0]^T$, $C_2^{'} = [-\frac{\sqrt{3}}{6}a, a/2, 0]^T$, and $C_3^{'} = [-\frac{\sqrt{3}}{6}a, -a/2, 0]^T$.

The origin coordinates of {m} in {B} are $\mathbf{o} = [o_x, o_y, o_z]^T$, and then $C_i = o + RC_i^{'}$ in {B}. As the actuated joints of the helical hand are all revolute joints, the axis of rotation of the segment C_iA_i is in the direction of OA_i at A_i, which makes the x-coordinate of the point C_1 is always equal to d, and similarly for the y-coordinate of the point C_2 and the z-coordinate of the point C_3. Then, the relationship between the object coordinates and the object orientation is given by

$$\mathbf{o} = \begin{bmatrix} o_x \\ o_y \\ o_z \end{bmatrix} = \begin{bmatrix} d - \frac{\sqrt{3}}{3}ar_{11} \\ d + \frac{\sqrt{3}}{6}ar_{21} - \frac{1}{2}ar_{22} \\ d + \frac{\sqrt{3}}{6}ar_{31} + \frac{1}{2}ar_{32} \end{bmatrix}. \quad (1)$$

where r_{ij} are the elements of the orientation matrix at the i-th row and the j-th column. Finally, from the component r_{32} of the orientation matrix R, the relationship between the size of the object a and the orientation of the object δ can be found, namely

$$-sin(\theta_2)cos(\delta + \pi/3) = \frac{C_{2z} - C_{3z}}{a}. \quad (2)$$

C. Helical Motion Determination

Based on the kinematic model of the manipulation phase, the trajectory of the grasped object can be worked out. The grasped object has a coupled rotation and translation movement when actuating the hand. For helical motion, the characteristic is that the centre of the object will move along the rotation axis while performing rotation. In this case, for different δ, the coordinates of those different $\mathbf{o}$ should follow along the rotation axis. It has been verified via numerical simulation in MATLAB that when all the three fingers' movements are identical, for different δ, the position of $\mathbf{o}$ moves along the vector $\vec{v} = [1\ 1\ 1]$, where the value of o_x, o_y, and o_z are all equal for each $\mathbf{o}$. In addition, the direction vector of the centre line (diagonal axis) of the hand is $\vec{v} = [1\ 1\ 1]$ as well in spatial frame. This result shows that the hand is able to manipulate an object under a helical motion along its diagonal axis.

Figure 3(b&c) illustrate the helical motion of a equilateral triangular object in two views under the actuation constraints. ψ indicates the object rotation range, the coloured circles denote the contact point positions, and the purple dots denote the centre points of the object. In the simulation, when plotted the translation distance vs time, the line is an approximately sine wave. In terms of the translation speed, it means objects will reach their maximum and minimum translation distances slowly and move relatively fast during the helical motion without considering the finger constraints.

From equation (1) and (2), it can be seen that the object size is one of the factors that effects the manipulation range and the grasping configuration of the helical hand. Fig. 4 illustrates the relationship amongst the object size, the hand configuration (α & β), and the object orientation (δ). It shows for a z axis helical motion controlled by two motors, when the object rotates anti-clockwise (δ increases), the proximal joints α_i will increase and the distal joints β_i will decrease. Green areas are the feasible rotation ranges for each size of object when actuation angle constraints are applied. Here the constraints are based on the helical hand design. The feasible rotation range (green shaded area) decreases significantly when the object size increases. Similarly, the translation distance o has been plotted with the object orientation δ in 4 different object sizes.

III. Control via Mechanical Intelligence

A. Two Motors Control

Since the contact point coordinates can be calculated by using the translation matrix and orientation matrix, the hand configuration can be defined through the inverse kinematics. If the coordinates of C_i are known, equation (3) will only has two sets of α_1 and β_1 values, which means each finger will have two configurations to grasp the object at the same position

$$\begin{cases} C_{1y} = l_1 cos\alpha_1 + l_2 cos(\alpha_1 + \beta_1) \\ C_{1z} = l_1 sin\alpha_1 + l_2 sin(\alpha_1 + \beta_1) \end{cases}. \quad (3)$$

Following these steps, given the moving trajectory of the object, when we keep α_1=α_2=α_3, if the results of β_i are the same ie. β_1=β_2=β_3, then we can say this hand mechanism

TABLE I

CONTROL RELATIONSHIP BETWEEN PROXIMAL JOINTS AND DISTAL JOINTS

object size	δ range	α initial	α final	$\Delta\alpha$	β initial	β final	$\Delta\beta$	$\Delta\beta/\Delta\alpha$	new $\Delta\beta$	new β final
30 mm	48° -76°	-16.1°	-3.2°	12.9°	95.5°	74.5°	21°	1.6279	18.9°	76.6°
40 mm	52° -70°	-18.8°	-7.5°	11.3°	92.6°	74.9°	17.7°	1.5663	16.6°	76.0°
50 mm	55° -66°	-20.5°	-11.1°	9.4°	88.4°	74.1°	14.3°	1.5212	13.8°	74.6°
60 mm	56° -63°	-21.6°	-15.2°	6.4°	83.5°	74.1°	9.4°	1.4687	10.4°	74.1°

Algorithm 1 Motor points calculation

procedure (REQUIRED JOINT ANGLES α,β)
  Compute Motor points $\mathbf{x_1}$ - Eq. (4)
  Compute the compliant distal angle $\beta_\mathbf{0}$ at $\mathbf{x_1}$ - Eq. (5)
  if $\beta_\mathbf{0} < \beta$ **then**
    β^+=β-$\beta_\mathbf{0}$
    Compute Motor points increment $\mathbf{x'_2}$ - Eq. (6)
    Motor points $\mathbf{x_2}$ = $\mathbf{x'_2}$+780
  else
    Motor points $\mathbf{x_2}$ remains at 780

Algorithm 2 Grasping & Manipulation Control Scheme

procedure (OBJECT SIZE $\mathbf{a}$, DESIRE ROTATION ANGLE δ OR TRANSLATION DISTANCE $\mathbf{o}$)
  Compute the initial grasping configuration $\alpha_{initial}$, $\beta_{initial}$ (joint angles) and $\mathbf{o}_{initial}$ (grasping height) based on the input object size $\mathbf{a}$ using equations (1&2)
  Compute the initial motor points (Algorithm 1)
  Move both motor to the calculated initial positions
  Compute the final grasping configuration α_{end}, β_{end} based on the input desire manipulation δ or $\mathbf{o}$ using equations (1) - (3)
  Compute the final motor points (Algorithm 1)
  Move both motors to the desired positions linearly to perform the manipulation

can perform the motion by using two motors, one for α joints, the other for β joints. Additionally, it can be shown using numerical simulation that when β_i are constrained to be equal, α_i can be the same to produce a helical motion along the object z axis based on the equation. This shows that the hand has the ability to perform the helical motion along the object z axis by only using two motors.

B. Helical Motion Control scheme

Both α_i and β_i in the green areas of Fig. 4 are approaching a linear trend for all sizes of objects. We analyzed the variation of α_i and β_i inside of the green shaded area in Table I to see how the changing rate of α_i and β_i varies with the object size. For different sizes of objects, the table shows the ratio between the $\Delta\beta$ (distal joints variation) and the $\Delta\alpha$ (proximal joints variation) are similar. The results show that the hand has potential to use the same speed control scheme to manipulate different sizes of objects. Higher ratio indicates greater change in the distal joints when changing the proximal joints. Therefore, in order to choose a suitable $\Delta\beta/\Delta\alpha$ ratio for a secure grasp during manipulation, the change in distal joints ($\Delta\beta$) can only be smaller than required. In this case, we chose the minimum $\Delta\beta/\Delta\alpha$ ratio which is the 60 mm object (1.4687) to calculate the new $\Delta\beta$. According to the results, the maximum difference between the $\Delta\beta$ and the new $\Delta\beta$ is 2.1°. Broadly speaking, the difference is not obvious in terms of the prototype, we can establish a hypothesis that this mechanical design is capable to perform a predictable in-hand helical motion of various object sizes at a constant speed (velocity regulation). The performance of the helical hand with velocity regulation by applying the new β final has been evaluated in the next section.

C. Practical control algorithm

For the practical case, due to the prototype design, the conversion between the joint angles (α_i, β_i) and the actuation motor positions is not straightforward. The distal links have a compliant adaptive motion while actuating the proximal links due to the compliant adaptive characteristic of the hand design. A motion tracking analysis has been operated to find out a mathematical way to implement the compliant adaptive motion. By just actuating the proximal joint motor and leaving the distal joint motor at its starting position (780 motor points in Arduino). Four markers were attached to the frame, the proximal joint, the distal joint and and the fingertip to record the variation of the joint angles (α_i, β_i) by actuating the proximal joint motor linearly. It is shown that within the proximal joint motor actuation range, the proximal joint angle α_i decreases from 7° to -48° and the distal joint angle β_i increases from 74° to 96° in an approximately linear way. By using the first order best fit function in MATLAB, *polyfit*, the function of joint angles (α_i, β_i) in terms of proximal joint motor's actuation points x_1 are

$$\alpha_i = -0.1194x_1 + 59.5236, \tag{4}$$

$$\beta_i = 0.0513x_1 + 48.2620, \tag{5}$$

where x_1 is between 450 and 900.

For in-hand manipulation or grasping complicated objects, the distal joints need an extra actuation of the distal joints motor. A similar motion tracking test was performed to find out the relationship between the β increment (β^+) and the distal joints motor points increment (x'_2)

$$\beta^+ = 0.1403x'_2 + 3.6448, \tag{6}$$

where x'_2 is between 0 and 220.

Here, Algorithm 1 describes the method of computing the motor points by inputting the required joint angles α and β based on the motion tracking's output equations.

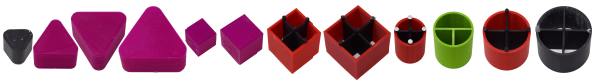

Fig. 5. 16 different testing objects for helical motion test: four triangles (30mm-60mm), four squares (30mm-60mm), and four cylinders (40mm-70mm).

TABLE II

SIMULATION AND EXPERIMENTAL RESULTS OF 3 OBJECT SHAPES ON VARIOUS SIZES WITH VELOCITY REGULATION CONTROL & MAXIMUM POSITION CONTROL SCHEME

	Simulation		Velcity Regulation		Maximum Position	
ob size	S: $\Delta\delta$	S: Δo	EV: ψ	EV: $\bar{o}$	EM: ψ	EM: $\bar{o}$
30 mm	27°	11.4	15.6°	10.6	20.7°	12.3
40 mm	17°	9.7	7.48°	8.77	20.5°	14.7
50 mm	11°	7.8	5.13°	7.81	10.6°	14.3
60 mm	6°	5.1	2.79°	4.71	5.86°	14.4

Algorithm 2, the manipulation control scheme, utilises the above motor points calculation to perform the helical or grasping manipulation.

IV. HELICAL MOTION PERFORMANCE

To evaluate the proposed control scheme of the helical hand, 12 different objects were manipulated by the helical hand (Fig. 5) with velocity regulation of actuators. The hand is facing up and holding the object firmly like Fig. 2(b). This setup configuration enables the cameras to record the markers properly. Each object has 4 tracking markers to define the centre and the edge of the object. Motion tracking cameras (OptiTrack Flex 3) were used to record the object trajectory. According to the new β_{final} from Table I and based on the control algorithms, the motors of the helical hand were set at the same speed to manipulate those 12 objects, size varies from 30mm to 60mm, in two conditions: direct and offset.

A. Helical Motion from Target Position

First condition is grasping the object at the centre of the hand and perform the manipulation with the constant velocity ratio followed by the control scheme. Table II shows the comparison of the simulation and the experimental rotation angle ψ ° and the translation distance o (mm). The simulation results are summarised from Table I and Fig. 4 and the experimental results are the average of all three object shapes. With the proposed velocity regulation control scheme, the helical hand can rotate and translate different objects at the same time. The experimental translation results are very close to the simulation range with error less than 1 mm. However, the experimental rotation results are less than the simulation results at around half of them.

Figure 6 illustrates the variation in rotation and translation of all triangular, square and cylinder objects in 4 different sizes. Due to the limitation on the rotation results, the experimental results are not quite match with the simulation trend. However, there are some objects follow the trend, e.g. the 60 mm triangle and circle etc. In summary, the triangular objects perform better than the others. This may because

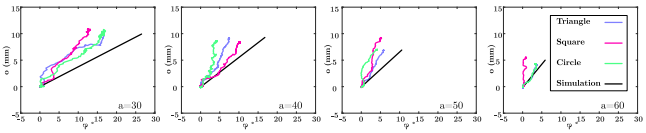

Fig. 6. The relationship between the translation distance o (mm) and the rotation ψ (°)with different object sizes on 3 different object shapes: triangles, squares, and circles. a is the size of the object in mm. The black lines are the simulation results and the rest coloured lines are the experimental results.

of the differences in grasping strategy for those three types of shapes. The contact locations are slightly different from those three shapes. Triangular objects have the best contact strategy as the hand topology is orthogonal. The hand grasps the cylinder in a similar strategy, but the contact condition is changing from a flat-to-flat contact to a flat-to-curved contact, the stability of the hand decreases. This may lead to tilting and slipping during the manipulation. For square objects, the grasping condition is different, the hand is incapable of holding the object evenly. So the hand is primarily using two fingers to grip the object and the rest finger for guiding the object or even providing a push out force towards to the fourth edge. This special grasping strategy limits the translation distance of the square objects.

To improve the rotation range of the hand, another experiment has been conducted to manipulate the same 12 objects but without using the velocity regulation control scheme. The control scheme is straightforward that controlling both motors to their maximum positions but this also has a drawback that the overload force may break the fingers. Table II last column shows the comparison of the simulation and the experimental results under this control scheme. The rotation ranges improved a lot on all object sizes where the differences are decreasing from average 7.5° to less than 1°, but the translation range became worse. The translation ranges have little changes among different sizes of objects, especially from size 40 mm to 60 mm, the average translation range are almost identical.

B. Helical Motion with Offset

Apart from grasping the object at the centre of the hand, we also tested the manipulation tolerance of the helical hand by placing the object at three offset positions. The offset positions are the positions of each fingertips at the opening stage. We labelled the first fingertip position as offset X, the second fingertip position as offset Y, and the third fingertip position as offset Z. The distal link adaptive feature are utilised in this experiments by grasping the object in offset positions. The helical hand was controlled under the velocity regulation control scheme for this experiments.

Figure 7 shows the rotation and translation range of both simulation and experimental results on all tested objects. The performance of each offset for different objects are not steady with the circle in offset Y position is the largest rotation of size 30 mm, and the square in offset Z position is the largest

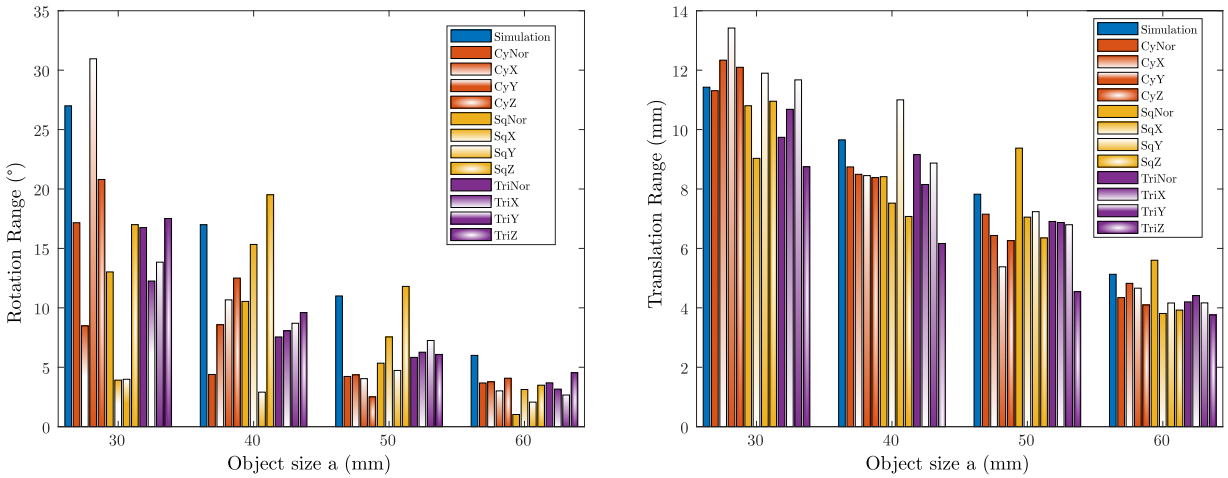

Fig. 7. Rotation and translation range of the experimental results for each object under direct and offset grasping. Different colours indicate different shapes and different infills indicate different grasping conditions. Blue denotes the simulation results, orange denotes the experimental results of circles, yellow for squares, and purple for triangles.

rotation of size 40 mm and 50 mm, but the average of all three offsets results are close to the direct grasping results. For object size 30 mm to 50 mm, the largest experimental rotation ranges are larger than the simulation results, but all experimental results for 60 mm objects are less than the simulation results.

The experimental results of translation ranges are more consistent and close to the simulation results. Fig. 7 shows for objects of size 30 mm, the translation ranges of offset Y position are the highest ones among other offset conditions. The translation ranges of offset Z position of triangular objects are the least for all sizes. Overall, the translation range differences among all three shapes at the same size are not obvious, the helical hand showed high manipulation capability and tolerance on translating objects regardless shape.

V. Discussion & Conclusion

Following the performance evaluation of the helical hand, it shows that the hand can manipulate objects in a helical motion with speed control and still keep the general grasping capabilities. The helical motion results verified the hand can rotate and translate an object at the same time with the simple speed control. Under the velocity regulation control scheme, for different object sizes and shapes, the velocities of both motors are always based on the same speed ratio. Due to the motor limitation, there is no torque control, the motors are position controlled indeed which are calculated from the simulation. As there is a reality gap and the manufacturing errors, the hand did not grasp the objects tight enough by using the calculated motor points. As shown in Table II with velocity regulation control, the rotation ranges are unsatisfactory due to the loose contact conditions and the backlash of the actuation gears. The trend of the manipulation capability are clear which is the rotation and the translation ranges decrease when the manipulated object sizes increase.

Moreover, we control the hand with the maximum control scheme, actuating the motors to their maximum positions, producing a very tight grasp during the manipulation, while delicate force may be required in the case of soft objects. Table II shows that the rotation ranges improve a lot compared to the previous method, but the translation ranges are unusual. As the motors are reaching to their maximum positions, the ended positions of the helical hand for most cases are similar, that is why the differences of the average translation ranges amongst various object sizes are close to each other. Furthermore, under the high grasping force, the proximal gears may jump over teeth when motors trying to reach their maximum positions due to the prototype manufacturing error.

One of the main issues during the potential application tests is the variation of the helical pitch for different tasks. With the velocity regulation control, the hand is only able to produce a certain type of helical motion which may not be able for all tasks. Nevertheless, the hand shows the capability to perform helical motion on different type of objects.

In summary, the proposed mechanical intelligence principle has been proved by the introduced prototype for helical prehensile in-hand manipulation on different types of objects. Under the simple velocity regulation control scheme, the proposed hand performs well enough on those tasks. Benefit from the differential system of the distal links, the helical hand shows good adaptive grasping and in-hand manipulation capability on error tolerance. Some potential improvements in the hand design are identified for future research. For example, adding springs to the linkages can increase the passive grasping forces. Furthermore, constraints on the distal links' ball joints will help prevent the fingertips from coming off. Additionally, if each proximal finger could be independently controlled to exhibit various in-hand manipulation behaviours, reincorporating with deep learning method, the grabbing ability and potential applications could significantly be increased.

REFERENCES

[1] OpenAI, M. Andrychowicz, B. Baker, M. Chociej, R. Józefowicz, B. McGrew, J. Pachocki, A. Petron, M. Plappert, G. Powell, A. Ray, J. Schneider, S. Sidor, J. Tobin, P. Welinder, L. Weng, and W. Zaremba, "Learning dexterous in-hand manipulation," *The International Journal of Robotics Research*, vol. 39, no. 1, pp. 3–20, 2020. [Online]. Available: https://doi.org/10.1177/0278364919887447

[2] OpenAI, I. Akkaya, M. Andrychowicz, M. Chociej, M. Litwin, B. McGrew, A. Petron, A. Paino, M. Plappert, G. Powell, R. Ribas, J. Schneider, N. Tezak, J. Tworek, P. Welinder, L. Weng, Q. Yuan, W. Zaremba, and L. Zhang, "Solving rubik's cube with a robot hand," *arXiv preprint*, 2019.

[3] A. Billard and D. Kragic, "Trends and challenges in robot manipulation," *Science*, vol. 364, no. 6446, p. eaat8414, 2019.

[4] L. Han and J. C. Trinkle, "Dextrous manipulation by rolling and finger gaiting," in *Proceedings. 1998 IEEE International Conference on Robotics and Automation (Cat. No. 98CH36146)*, vol. 1. IEEE, 1998, pp. 730–735.

[5] K. Nagata, "Manipulation by a parallel-jaw gripper having a turntable at each fingertip," in *Proceedings of the 1994 IEEE International Conference on Robotics and Automation*. IEEE, 1994, pp. 1663–1670.

[6] M. Grebenstein, A. Albu-Schäffer, T. Bahls, M. Chalon, O. Eiberger, W. Friedl, R. Gruber, S. Haddadin, U. Hagn, R. Haslinger, H. Höppner, S. Jörg, M. Nickl, A. Nothhelfer, F. Petit, J. Reill, N. Seitz, T. Wimböck, S. Wolf, T. Wüsthoff, and G. Hirzinger, "The dlr hand arm system," in *2011 IEEE International Conference on Robotics and Automation*. IEEE, 2011, pp. 3175–3182.

[7] H. Kawasaki, T. Komatsu, and K. Uchiyama, "Dexterous anthropomorphic robot hand with distributed tactile sensor: Gifu hand ii," *IEEE/ASME transactions on mechatronics*, vol. 7, no. 3, pp. 296–303, 2002.

[8] Shadow, *Shadow Dexterous Hand*, Shadow Robot Company, 2019. [Online]. Available: https://www.shadowrobot.com/products/dexterous-hand

[9] M. Ciocarlie, F. M. Hicks, R. Holmberg, J. Hawke, M. Schlicht, J. Gee, S. Stanford, and R. Bahadur, "The velo gripper: A versatile single-actuator design for enveloping, parallel and fingertip grasps," *The International Journal of Robotics Research*, vol. 33, no. 5, pp. 753–767, 2014.

[10] A. M. Dollar and R. D. Howe, "Joint coupling design of underactuated hands for unstructured environments," *The International Journal of Robotics Research*, vol. 30, no. 9, pp. 1157–1169, 2011.

[11] G. Bai and N. Rojas, "Self-adaptive monolithic anthropomorphic finger with teeth-guided compliant cross-four-bar joints for underactuated hands," in *2018 IEEE-RAS 18th International Conference on Humanoid Robots (Humanoids)*. IEEE, 2018, pp. 145–152.

[12] H. Stuart, S. Wang, O. Khatib, and M. R. Cutkosky, "The ocean one hands: An adaptive design for robust marine manipulation," *The International Journal of Robotics Research*, vol. 36, no. 2, pp. 150–166, 2017.

[13] K. Hang, W. G. Bircher, A. S. Morgan, and A. M. Dollar, "Hand–object configuration estimation using particle filters for dexterous in-hand manipulation," *The International Journal of Robotics Research*, p. 0278364919883343, 2019.

[14] Q. Lu, N. Baron, G. Bai, and N. Rojas, "Mechanical intelligence for adaptive precision grasp," in *2021 IEEE International Conference on Robotics and Automation (ICRA)*. IEEE, 2021, pp. 4530–4536.

[15] N. Rojas and A. M. Dollar, "Gross motion analysis of fingertip-based within-hand manipulation," *IEEE Transactions on Robotics*, vol. 32, no. 4, pp. 1009–1016, 2016.

[16] I. M. Bullock, R. R. Ma, and A. M. Dollar, "A hand-centric classification of human and robot dexterous manipulation," *IEEE transactions on Haptics*, vol. 6, no. 2, pp. 129–144, 2012.

[17] N. Rojas, R. R. Ma, and A. M. Dollar, "The gr2 gripper: an underactuated hand for open-loop in-hand planar manipulation," *IEEE Transactions on Robotics*, vol. 32, no. 3, pp. 763–770, 2016.

[18] C. Della Santina, C. Piazza, G. Grioli, M. G. Catalano, and A. Bicchi, "Toward dexterous manipulation with augmented adaptive synergies: The pisa/iit softhand 2," *IEEE Transactions on Robotics*, vol. 34, no. 5, pp. 1141–1156, 2018.

[19] H. Liu, Z. Zhang, X. Zhu, and K. Xu, "A single-actuator gripper with a working mode switching mechanism for grasping and rolling manipulation," in *2018 IEEE/ASME International Conference on Advanced Intelligent Mechatronics (AIM)*. IEEE, 2018, pp. 359–364.

[20] Q. Lu, N. Baron, A. B. Clark, and N. Rojas, "Systematic object-invariant in-hand manipulation via reconfigurable underactuation: Introducing the ruth gripper," *The International Journal of Robotics Research*, vol. 40, no. 12-14, pp. 1402–1418, 2021.

[21] L. U. Odhner and A. M. Dollar, "Dexterous manipulation with underactuated elastic hands," in *2011 IEEE international conference on robotics and automation*. IEEE, 2011, pp. 5254–5260.

[22] A. Bicchi and R. Sorrentino, "Dexterous manipulation through rolling," in *Proceedings of 1995 IEEE International Conference on Robotics and Automation*, vol. 1. IEEE, 1995, pp. 452–457.

[23] J. Zhou, J. Yi, X. Chen, Z. Liu, and Z. Wang, "Bcl-13: A 13-dof soft robotic hand for dexterous grasping and in-hand manipulation," *IEEE Robotics and Automation Letters*, vol. 3, no. 4, pp. 3379–3386, 2018.

[24] A. Nagabandi, K. Konoglie, S. Levine, and V. Kumar, "Deep dynamics models for learning dexterous manipulation," *arXiv preprint arXiv:1909.11652*, 2019.

[25] L. U. Odhner, L. P. Jentoft, M. R. Claffee, N. Corson, Y. Tenzer, R. R. Ma, M. Buehler, R. Kohout, R. D. Howe, and A. M. Dollar, "A compliant, underactuated hand for robust manipulation," *The International Journal of Robotics Research*, vol. 33, no. 5, pp. 736–752, 2014.

[26] B. A. Kent, N. Karnati, and E. D. Engeberg, "Electromyogram synergy control of a dexterous artificial hand to unscrew and screw objects," *Journal of neuroengineering and rehabilitation*, vol. 11, no. 1, p. 41, 2014.

[27] N. Karnati, B. A. Kent, and E. D. Engeberg, "Bioinspired sinusoidal finger joint synergies for a dexterous robotic hand to screw and unscrew objects with different diameters," *IEEE/ASME Transactions on Mechatronics*, vol. 18, no. 2, pp. 612–623, 2012.

[28] B. Shih, D. Drotman, C. Christianson, Z. Huo, R. White, H. I. Christensen, and M. T. Tolley, "Custom soft robotic gripper sensor skins for haptic object visualization," in *2017 IEEE/RSJ international conference on intelligent robots and systems (IROS)*. IEEE, 2017, pp. 494–501.

[29] H. Zhu, A. Gupta, A. Rajeswaran, S. Levine, and V. Kumar, "Dexterous manipulation with deep reinforcement learning: Efficient, general, and low-cost," in *2019 International Conference on Robotics and Automation (ICRA)*. IEEE, 2019, pp. 3651–3657.